Photo-Textured Rendering of Developable Surfaces in Architectural Photogrammetry

George E. Karras[1], Elli Petsa[2], Amalia Dimarogona[1], Stefanos Kouroupis[2]

[1] Laboratory of Photogrammetry, National Technical University of Athens, Greece
[2] Department of Surveying, Technological Educational Institute of Athens, Greece

Abstract. New techniques constantly seek to meet a growing demand for realistic photo-textured 3D models in architecture and archaeology. When only visualisation is required, the emphasis lies on visual quality rather than accuracy. But in architectural photogrammetry the primary requirement is mostly to produce accurate mappings under strict specifications. Hence, accuracy comes first; yet visual products can benefit from precise modeling. In this context, a treatment of cylindrical and conic surfaces is presented. The process for developing them onto the plane (the basic way to represent such surfaces) is outlined and illuminated at the example of two large ancient towers in the framework of projects prepared for the Greek Ministry of Culture. But besides their metric utility, these products represent ideal photo-textures for draping the mathematical surface to generate virtual reality effects. The results of such successful photorealistic visualisations are presented and discussed.

1 Introduction

We are currently witnessing a growing demand for virtual representations in architecture and archaeology, e.g. in virtual tourism or architectural walk-throughs. This demand mainly focuses on the use of real-scene image content to create animated photo-textured 3D models. The platform-independent and web-oriented VRML data format is widely used for viewing texture-mapped models with freeware browsers. These visual models allow to create images from any possible viewing angle, providing views very similar to those perceived by the human eye. More sophisticated techniques, like the visibility preprocessing through construction of view maps [1], facilitate the quick and realistic generation of novel scene views.

Indeed, there exist instances where simply a visualisation will suffice. In this case, image-based rendering techniques may be adopted [2]; however, their lack of geometric model disturbs the freedom to render from arbitrary viewpoints and hinders accuracy [3]. What is more important, geometric modeling itself basically represents the actual requirement since, as a rule, photogrammetry is called upon not just to render, visualise, 'virtualize' or animate but, above all, to *map* objects of architectural / archaeological significance according to strict specifications. Whether in the context of geometric documentation or that of restoration, these specifications are to be totally adhered to, particularly regarding the scale of the deliverables and, hence, their accuracy. In this sense, 3D photo models – in which the stress generally lies on visual quality and realistic impression rather than accuracy – are mostly a secondary product of architectural photogrammetry.

Several approaches for 3D capturing and modeling are being developed recently. Among such approaches, which display varying levels of automation and potential for capturing detail, none appears as suitable for the demands of all applications [3]. At the one end of image-based techniques one finds standard photogrammetric approaches, realised as commercial software and typically involving control points, bundle adjustment and interactive digitisation (with or without stereo-viewing). At the other end, one encounters today's fully automatic computer vision approaches based on video sequences and matching algorithms to extract 3D scene structures using solely the image contents, i.e. without prior information regarding object or calibration [4, 5]. Despite their obvious merits and potential, such approaches seem at present to be limited to particular applications, objects, environments and accuracy performances, mainly due to their need for densely taken images with similar viewpoints and the related sensitivity to noise [3, 6]. In fact, most people with a practical experience in actual projects of architectural photogrammetry would recognise a severe limitation in this need for successive images taken closely to each other. This may be impossible in many outdoor instances (like those treated here), e.g. when images have to be taken from the tops of neighbouring buildings or from platforms such as camera elevators, scaffolds, tripods – in short, when a continuous all-around recording of the object with a moving camera, in a controlled or a free manner, is out of the question. Besides, analogue cameras are preferred in many projects thanks to their image quality and flexibility in focal lengths, and hence image scales, compared to video recordings. It seems, however, that several "short baseline" problems are indeed tackled by the automatic self-calibration techniques which handle wider baseline stereo and large differences in interior orientation [7]. It appears that this kind of approach is more "universal" for architectural photogrammetry – provided its accuracies have been tested under practical conditions.

Between the above two lines of approach, one finds systems starting with a coarse 3D model, created interactively, which is then subjected to automatic image-based refinement [1, 8]. Thanks to the a priori geometric constraints, a smaller number of images are required. This approach is apparently restricted to typical, and not too complex, architectural ensembles which can be approximated by combinations of 3D primitives. Although the reconstruction algorithm does not recover surfaces of revolution and requires calibrated cameras, this approach could, in principle, be suitable for the cylindrical and conic surfaces treated here. In the present contribution, the problem has been confronted through an interactive single-image mapping technique based on prior knowledge of the mathematical solids (determined from surveyed points). Only circular cylinders and cones have been treated here, but the technique could be extended to include further analytical solids. On the other hand, "random" developable surfaces (such as a vertical wall with an arbitrary directing curve) call for a different approach.

2 The photogrammetric treatment of regular surfaces

For obvious reasons, monoscopic techniques are preferred in photogrammetric practice whenever possible. Purely "monocular" methods are essentially employed in three instances. First, for surfaces which are basically planar; indeed, 'rectification' remains the most popular photogrammetric tool for archaeological and architectural mapping. Second, for polyhedral objects, in which cases single perspective views can be handled successfully and displayed as 3D photo-textured models (see links in [9]). Finally, for objects with smooth surfaces which may be approximated analytically by quadrics, a surface type not at all rare in terrestrial photogrammetry. Indeed, among such cylindrical, conic, spherical, parabolic or ellipsoidal surfaces often encountered in close-range projects, one would count ancient theatres and tombs; parts of churches, monasteries and factories; towers, lighthouses, aqueducts, mills and chimneys; cupolas, rotundas, domes, vaults, arches and ceilings. These surfaces vary in size and are found in urban environments, in the countryside, in interior settings, above ground or even underground.

In a different context it can be assumed that, given a surface shape and its parameters, additional points can be interpolated to densify the triangulated surface [3]. Here, on the other hand, all processing is done with the analytical equation itself. Thus, after fitting to redundant surface points, the fundamental idea for single-image mapping of such objects is to 'intersect' their analytical expression with the projective bundle of rays to obtain space coordinates of the digitised points [10].

2.1 Surface fitting

Best-fitting solids are usually determined by least-squares fitting to surface points measured geodetically or photogrammetrically (for smooth surfaces, the quadric outlines may also be exploited in this respect [11]). If surface type is not obvious, a full 2^{nd} order equation of nine independent unknowns is fitted to the 3D point set. The coefficients incorporate the three parameters of the 'canonical form' defining shape (surface type) and size, and six elements of rigid body transformation fixing position and orientation in the coordinate system (on the use of surface invariants to classify quadrics see [12]). Besides surface parameters, fitting processes must also yield point deviations from the fitted surface. Depending on the algorithm, the residuals are either in the directions of the coordinate axes or normal to the surface.

2.2 Mapping of regular surfaces

As a rule, users (architects, archaeologists, conservationists) wish to have a scaled map delivered for measuring purposes. But how to represent such a steeply curving surface? Obviously, users will reject a conventional orthogonal projection which appears to vary in scale in one direction and "fades away" rapidly at the sides. In fact, it is mostly required that cylinders and cones are developed ('unwrapped' or 'unfolded') onto a plane. The non-developable surfaces (mostly spheres) should be ‘flattened’ into suitable cartographic projections. Indeed, this is practically the only option available for the metric representation of regularly curved surfaces.

For raster products, the mapping process is as follows. Let **M** denote the transformation (development or cartographic projection) of the 3D surface coordinates **X** to the transformed 2D system $\mathbf{X}_T$, and **P** denote the projective relation of image point **x** to the space point **X**:

$$\left(\mathbf{X}_T = \mathbf{MX} \quad \text{and} \quad \mathbf{x} = \mathbf{PX} \right) \;\rightarrow\; \mathbf{x} = \mathbf{PM}^{-1}\mathbf{X}_T$$

The transformed position $\mathbf{X}_T$ is thus related to the corresponding image position **x**, which allows to resample the transformed image. Basic steps for surface development include: selection for each particular image of a corresponding object area to be developed; transformation **M** defines an equivalent area in the X_TY_T system; the pixel size in ‘developed space’ X_TY_T is chosen according to the required scale of mapping and fixes the size of the final image; each pixel of the latter uniquely defines an object point XYZ via the inverse transformation $\mathbf{M}^{-1}$; a 3D–2D back projection **P** leads to the corresponding location on the original image. All images thus resampled are adapted radiometrically and merged into a “developed” mosaic to produce the end product of surface unwrapping [10, 13].

Projection of non-developable surfaces proceeds in a similar manner. Yet, the basic difference lies in the fact that the choice of the particular projection is not a trivial task, depending on the needs of the user (should it be conformal or equidistant, or should it simply “look real”?). Such an application has been reported in [13].

2.3 Accuracy considerations

Locally, the accuracy of projection depends strongly on the angle of intersection of a projective ray with the surface. Small angles propagate unfavourably the orientation errors to the mapping result. This is equally true for the effect of local deviations from the best-fitting surface (which is a serious problem since the smoothness of an actual surface is rarely perfect). Therefore, when planning photography one must fix a limit for the angle of intersection to define an acceptable working area on the image. Areas of local deviation from the solid should be imaged frontally, whenever possible. Generally, cylindrical or conic objects have to be covered from at least six view points, evenly distributed around them. As a rule, normal lenses should be preferred against wide-angle lenses [10].

3 Practical application with two ancient towers

3.1 The objects: description, limitations and geodetic control

Here, a short description of the application is given (more details are given in [14]). The Greek Ministry of Culture required the documentation of the exterior surface of two archaeologically important monuments of the Hellenistic period (circa 300 B.C.), both situated on islands of the Aegean. The *Drakanos* tower, on the island of Ikaria, is 12 m high and has a cylindrical shape with an external diameter of 8.5 m (Fig. 1). The conic tower of *Ag. Petros*, on the island of Andros, is larger: its height reaches 19 m above ground; its diameter is 10 m at base level; the inclination of its generatrices against the vertical is 2.6° (Fig. 2).

Figure 1. The cylindrical Drakanos tower on the island of Ikaria (left: the adjusted fishing rod used for photography).

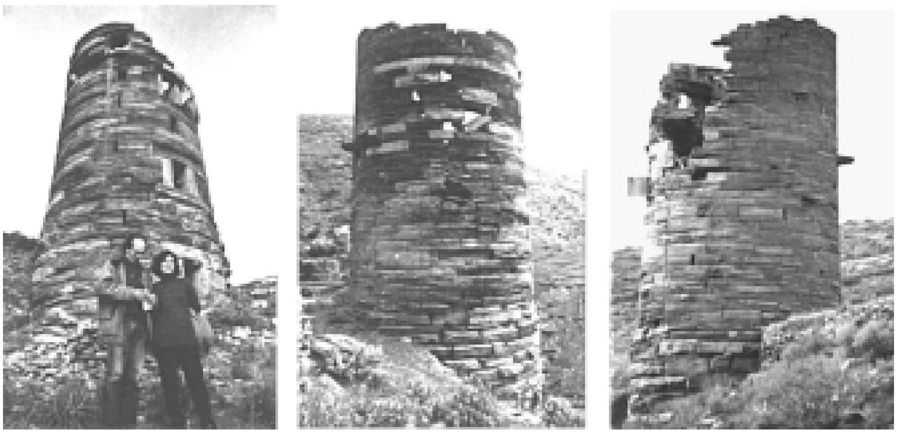

Figure 2. The conic tower of Ag. Petros on the island of Andros.

Both objects have suffered severe damage through time (gaps, displaced stones and erosion). Raster developments of the exterior surfaces were needed in a 1:25 scale, although it was recognised that accuracies no better than 3 cm could be expected due to the rough relief of the surface itself. The size, shape and location of the monuments posed several problems with direct impact on the approach to be adopted:

- The objects had considerable localised deviations from a perfectly smooth solid. This called for a relatively dense photographic coverage to minimize perspective distortions and occlusions.
- As the Drakanos tower is located on relatively flat terrain, the camera had to be somehow raised for frontal recording (which excluded metric or réseau cameras due to their weight). The terrain around the Ag. Petros tower slopes steeply. To make things worse, both objects are in totally isolated areas, accessible only on foot. This excluded the employment of mechanical means for raising a camera. Finally, as image acquisition had to take place in mid-winter, the anticipated winds of the Aegean ruled out the use of a 'flying' camera platform like the small meteorological balloon successfully used in other cases [15]. These difficulties in image acquisition also had the following consequence.
- In principle, one might have used minimal ground control and bundle adjustment to simultaneously recover camera exterior orientations and surface points for surface fitting. But this would require more image coverage than absolutely necessary for mapping. More important, a variety of cameras, lenses and zooms had to be employed. A bundle adjustment with so many 'block-variant' interior orientation parameters would be a problem in itself. It was simpler to geodetically measure natural detail points on the surface.

Thus, a large number of detail points were surveyed with an estimated precision of 3 cm (mainly attributed to uncertainties in identification). Then, having established first that the surfaces were indeed what "they looked like", namely right circular, surface fitting gave the results of Table 1.

Table 1. Results of surface fitting

	Drakanos Tower	Ag. Petros Tower
Shape	Cylinder	Cone
Number of points	91	208
Radius (m)	4·210 ± 0·007	–
Elevation of the vertex above threshold (m)	–	107·766 ± 1·646
Angle β of generatrices against the vertical (º)	–	2·592 ± 0·044
Planimetric precision of the vertical axis (m)	$\sigma_X = \sigma_Y = \pm 0{\cdot}010$	$\sigma_X = \sigma_Y = \pm 0{\cdot}005$
RMS deviation normal to the surface (m)	0·068	0·052

Results show that the cylinder is defined precisely. The somewhat large RMS value is due to points having been measured both on the embossed faces of the stones and their joints to produce a best mean fit. A high planimetric precision is also obtained for the vertex of the cone. On the other hand, its small angle, coupled with an elevation range (~20 m) which is but a small fraction of the total height of the mathematical solid above ground (~110 m), understandably gave a large standard deviation for the elevation of the vertex. Of course, this value is extremely highly correlated with that of angle β, in other words their "combination" precisely approximates shape and size of the *actually existing* range of the cone.

3.2 Photography

As mentioned, light non-metric cameras were to be used. In view of the expected accuracy of 3 cm, the negative scale was to be kept above 1:350.

For the Drakanos tower the camera had to be raised. To this end, an adapted telescopic fishing-rod was extended with aluminium bars to reach a maximum height of 9 m above ground level; the light small format camera was mounted on top with horizontal imaging axis (Fig. 1, left). Its normal and wide-angle lenses were used. Thanks to this device the monument was fully covered in two overlapping “circular strips” from 8 different viewpoints. Despite the wind, images of good quality were acquired.

Being considerably higher and located on sloping terrain, the conic tower could not be imaged with this camera platform. A substantial part of this object was recorded at close range from higher spots of the ascending ground using a medium format camera and wide-angle, normal and zoom lenses. For the rest of the object the only alternative left was to exploit the surrounding hills using very large focal lengths. A small format camera was employed with a 300 mm telephoto lens enhanced with two teleconverters (1.6× and 2×). This combination allowed a maximal focal length equivalent to almost 1 m and imaging distances reaching 350 m. Despite certain degradations of image quality due to haze, the images were sufficiently sharp for the specific purpose. With this camera / lens combination, we finally managed to cover the monument in two “circular strips” from 7 directions.

3.3 Photogrammetric processing

A total of 17 and 14 photographs were selected for the Drakanos and the Ag. Petros towers, respectively, scanned at appropriate resolutions to accommodate the pixel size of the deliverables (2.5 mm in “developed” object space). Except for the radial distortion polynomial of the wide-angle lens, known beforehand via self-calibration, no information on interior orientation was available. The Direct Linear Transformation (DLT) algorithm is best suited for such cases, an approach establishing direct projective 2D-3D relations between image and object [16]. The control information with adequate extension in depth needed in the DLT approach was available thanks to the marked surface curvatures.

The selected images were then developed using the DLT results (images from the wide-angle lens were corrected for radial distortion during resampling). Since the ‘unfolded’ images did not exactly fit with each other, mosaicking was geometrically perfected by manual editing over the background of “developed” control points. Whenever possible, the displacements due to relief or the occlusions were locally corrected from frontal detail images. The final products, adapted radiometrically into uniform grey-scale mosaics and actually delivered as 1:25 prints on photographic paper, are presented in Figs. 3 and 4.

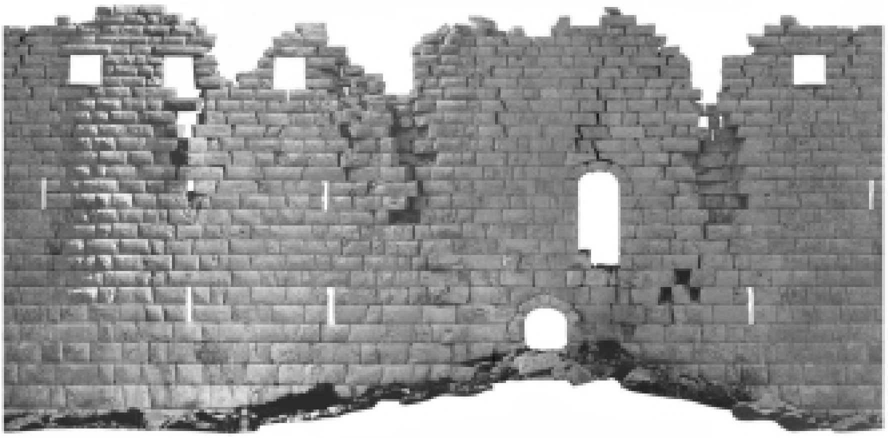

Figure 3. The development of the cylindrical tower of Drakanos.

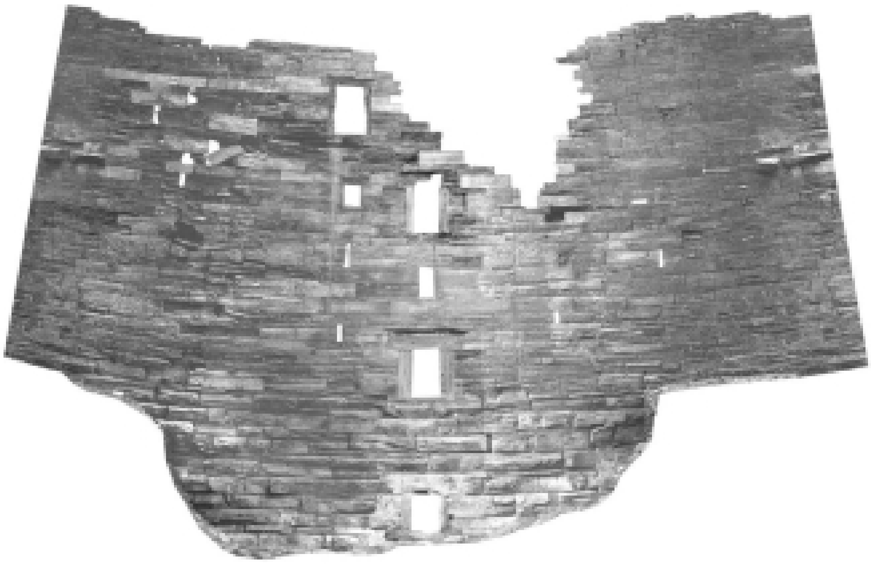

Figure 4. The development of the conic tower of Ag. Petros.

3.4 Accuracy assessment

The final accuracy of development was assessed through affine transformations between mosaics and the “developed” control points. The resulting RMS deviations of 3-4 cm were regarded as satisfactory by the end-users (who were actually very impressed by such large-scale products new to them). Inaccuracies are larger in the ‘stretched’ horizontal direction of development, in which the presence of small remaining perspective distortions is more significant. Furthermore, in the areas of localised deformation stones had been slightly moved and scaled to occupy what was considered as their "proper" place. Thus, the estimated accuracy refers solely to measured points assumed to lie on a smooth surface in order to be developed. Although (thanks to the large number and good distribution of points checked) the estimated accuracy is regarded as representative for the whole object, local inaccuracies in areas of 3D deformation cannot be fully assessed. This appears to be an inevitable cost paid to unfold surfaces with certain deviations from a mathematical solid. Yet, as already noted, the main task was not to measure deformation (which would clearly call for a different approach) but to map the undeformed areas, to which the damaged parts should be adapted at the restoration phase.

4 Photo-textured rendering of the surfaces

Besides their metric property, the images of Figs. 3, 4 are also a form of visualisation to facilitate understanding and communication. However, a more straightforward type of presentation and visual impression can be created through the generation of VRML models. This format is viewed with freely available browsers and allows user-friendly interactive visualisation, which represent serious advantages if the results are addressed to people who may be unfamiliar with this type of data manipulation (such is the case with most archaeologists). In this respect, the photographic texture of the surface development mosaics assumes a further importance.

Terrain morphology used for the creation of the 3D models has been modeled from ground points measured geodetically. The insertion of the solids was subsequently programmed in VRML using their 3D base coordinates and their height, followed by small adaptations to fit local micro-relief. Regarding photo-texture, real-scene images are obviously subject to perspective distortions, which need to be corrected prior to draping. In general, this means that image-textures have to be transformed to orthogonal projections. In the present case, however, an orthogonal projection is rather meaningless. Instead, the "unfolded" images of Figs. 3, 4 actually represent suitably transformed textures for surface draping. While the content of the cylinder development of Fig. 3 has an orthogonal shape and can be draped without problem, the shape of the 'unwrapped' cone of Fig. 4 is curved. Hence, it had to be 'unbent' to fit perfectly the conic solid. To this end, its development was produced with each horizontal section unfolded in a different scale to yield the same perimeter.

Furthermore, all openings, missing parts and gaps had to be made transparent to allow unobstructed observation from any direction and viewing of the interior. No real images were at hand for the inner walls which were given the texture of the outer surface. Finally, a realistic wall thickness effect was created by a dense duplication of the surfaces. The resulting 3D models convey a realistic impression which is regarded as very satisfactory and was appreciated by the end-users. Selected views of the virtual models are to be seen in Figs. 5 and 6.

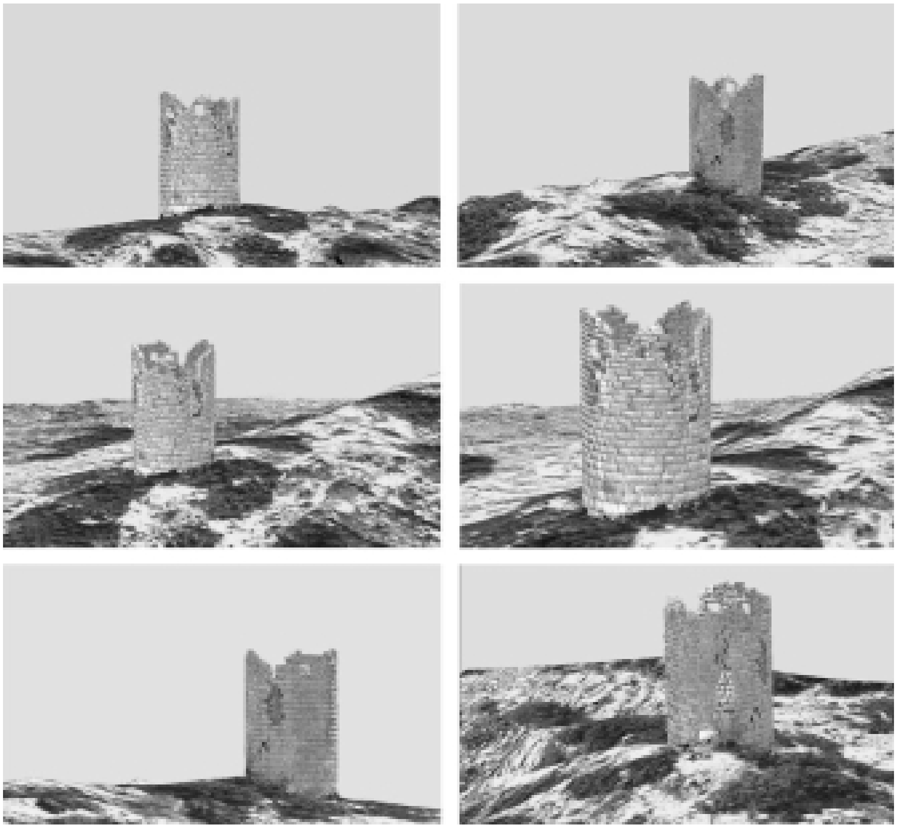

Figure 5. Frames of the virtual 3D model of the Drakanos tower and environment.

5 Conclusion

Thanks to digital techniques, architectural photogrammetry appears in recent years as more efficient and inexpensive, with simple cameras being successfully used in PC-based production of high quality visual deliverables. Unlike conventional line drawings, such approaches reproduce the pictorial wealth of the original images. In this context, the single-image approach presented and illustrated at the example of two ancient towers allows to map cylindrical and conic surfaces in the form of mosaicked digital developments. Additionally, however, an end-user often finds 3D visualizations not simply impressive but also very useful as overall views of the site or monument, or as possible visual information open to the public. Pictorial photogrammetric products of high metric quality thus represent an excellent 'pre-processed' photo-material for draping 3D models to generate virtual reality effects. Besides rectified images and orthophotographs, commonly used in this context, the developed imagery presented here may be successfully used to generate 3D photo-realistic visualisations. Skew surfaces, basically transformed to cartographic projections, need also to be investigated in this context.

Figure 6. Frames of the virtual 3D model of the conic Ag. Petros tower and environment.

As a final general statement, one should repeat that the primary concern of architectural photogrammetry is accuracy of reconstruction and presentation. Basically oriented towards automation and visualization, many publications reporting image-based 3D modeling methods rarely appear to address issues of geometric accuracy of the model [3]. Furthermore, one should add, the objects of a photogrammetric project are real objects, each posing its own geometric difficulties such as those described in this contribution. From a photogrammetrist's point of view, it is very important to expect a closer combination of the experimental wealth, algorithmic power and innovative perspectives of computer vision and computer graphics with the more practical aspects and considerations of current photogrammetric practice.

References

1. Debevec P, Yu Y, Borshukov G (1998). *Efficient View-Dependent Image-Based Rendering with Projective Texture-Mapping*, Technical Report UCB//CSD-98-1003, University of California at Berkeley.
2. Kang SB (1999). A survey of image-based rendering techniques. *Videometrics VI*, Proc. SPIE, 3641:2-16.

3. El-Hakim S (2000). A practical approach to creating precise and detailed 3D models from single and multiple views. *Int. Arch. Phot. Rem. Sens.,* 33(5):204-210
4. Pollefeys M, Koch R, Vergauwen M, Van Gool L (1999). An automatic method for acquiring 3D models from photographs: applications to an archaeological site. *Int. Arch. Phot. Rem. Sens.,* 32(5):76-80.
5. Zisserman A, Fitzgibbon A, Cross G (1999). VHS to VRML: 3D graphical models from video sequences. *Proc. IEEE Int. Conf. on Multimedia and Systems*, Florence, pp.51-57.
6. Varshosaz M, Dowman I, Chapman D (2000). Towards automatic reconstruction of visually realistic models of buildings. *Int. Arch. Phot. Rem. Sens.,* 33(5):180-186.
7. Pritchett P, Zisserman A (1998). Wide baseline stereo matching. *Proc. 6th ICCV*, Bombay, India, pp. 754-760.
8. Debevec P, Taylor CJ, Malik J (1996). Modeling and rendering architecture from photographs: a hybrid geometry and image-based approach, *Proc. ACM SIGGPAPH '96*, pp. 11-20.
9. http://info.uibk.ac.at/sci-org/cipa/tg2_1.html. CIPA Task Group 2 on "Single Images in Conservation" (accessed March 31, 2001).
10. Karras GE, Patias P, Petsa E (1996). Monoplotting & photo-unwrapping of developable surfaces in architectural photogrammetry. *Int. Arch. Phot. Rem. Sens.*, 31(5):290-294.
11. Cross G, Zisserman A (1998). Quadric reconstruction from dual-space geometry. *Proc. 6th ICCV*, Bombay, India, pp. 25-31.
12. Theodoropoulou I (2000). The definition of reference surfaces for architectural photogrammetry. *Int. Arch. Phot. Rem. Sens.,* 33(5):830-837.
13. Karras GE, Patias P, Petsa E, Ketipis K (1997). Raster projection and development of curved surfaces. *Int. Arch. Phot. Rem. Sens.*, 32(5C1B):179-185.
14. Theodoropoulou I, Petsa E, Karras GE (2001). Digital surface development of large cylindrical and conic structures with a single-image technique. *Phot. Rec.* 17(97), in print.
15. Karras GE, Mavromati D, Madani M et al. (1999). Digital orthophotography in archaeology with low-altitude non-metric images. *Int. Arch. Phot. Rem. Sens.*, 31(5W11):8-13.
16. Abdel-Aziz YI, Karara HM (1971). Direct linear transformation from comparator coordinates into object space coordinates in close-range photogrammetry. *ASP Symp. on Close-Range Photogrammetry*, Falls Church, Virginia, pp. 1-18.